Biochemical Pharmacology 83 (2012) 406–418

Contents lists available at SciVerse ScienceDirect

Biochemical Pharmacology

journal homepage: www.elsevier.com/locate/biochempharm

A-1048400 is a novel, orally active, state-dependent neuronal calcium channel blocker that produces dose-dependent antinociception without altering hemodynamic function in rats

Victoria E. Scott *, Timothy A. Vortherms, Wende Niforatos, Andrew M. Swensen, Torben Neelands, Ivan Milicic, Patricia N. Banfor, Andrew King, Chengmin Zhong, Gricelda Simler, Cenchen Zhan, Natalie Bratcher, Janel M. Boyce-Rustay, Chang Z. Zhu, Pramila Bhatia, George Doherty, Helmut Mack, Andrew O. Stewart, Michael F. Jarvis

Global Pharmaceutical Research and Development, Abbott Laboratories, 100 Abbott Park Road, Abbott Park, IL 60064, USA

ARTICLE INFO

Article history:
Received 29 September 2011
Accepted 31 October 2011
Available online 16 November 2011

Keywords:
N-type Ca^{2+} channels
T-type Ca^{2+} channels
Dorsal root ganglion
Neuropathic pain
Nociceptive pain
A-1048400

ABSTRACT

Blockade of voltage-gated Ca^{2+} channels on sensory nerves attenuates neurotransmitter release and membrane hyperexcitability associated with chronic pain states. Identification of small molecule Ca^{2+} channel blockers that produce significant antinociception in the absence of deleterious hemodynamic effects has been challenging. In this report, two novel structurally related compounds, A-686085 and A-1048400, were identified that potently block N-type (IC_{50} = 0.8 μM and 1.4 μM, respectively) and T-type (IC_{50} = 4.6 μM and 1.2 μM, respectively) Ca^{2+} channels in FLIPR based Ca^{2+} flux assays. A-686085 also potently blocked L-type Ca^{2+} channels (EC_{50} = 0.6 μM), however, A-1048400 was much less active in blocking this channel (EC_{50} = 28 μM). Both compounds dose-dependently reversed tactile allodynia in a model of capsaicin-induced secondary hypersensitivity with similar potencies (EC_{50} = 300–365 ng/ml). However, A-686085 produced dose-related decreases in mean arterial pressure at antinociceptive plasma concentrations in the rat, while A-1048400 did not significantly alter hemodynamic function at supra-efficacious plasma concentrations. Electrophysiological studies demonstrated that A-1048400 blocks native N- and T-type Ca^{2+} currents in rat dorsal root ganglion neurons (IC_{50} = 3.0 μM and 1.6 μM, respectively) in a voltage-dependent fashion. In other experimental pain models, A-1048400 dose-dependently attenuated nociceptive, neuropathic and inflammatory pain at doses that did not alter psychomotor or hemodynamic function. The identification of A-1048400 provides further evidence that voltage-dependent inhibition of neuronal Ca^{2+} channels coupled with pharmacological selectivity vs. L-type Ca^{2+} channels can provide robust antinociception in the absence of deleterious effects on hemodynamic or psychomotor function.

Abbreviations: A-686085, (1-(2-(4-(3,5-dimethoxybenzyl)piperazin-1-yl)ethyl)-3,3-bis(4-fluorophenyl)pyrrolidin-2-one); A-1048400, (1-[2-(4-benzhydryl-piperazin-1-yl)-2-oxo-ethyl]-3,3-diphenyl-piperidin-2-one); MW, molecular weight; FLIPR, fluorometric imaging plate reader; DRG, dorsal root ganglion; HEK, human embryonic kidney; HBSS, hanks balanced salt solution; CCI, chronic constriction injury; SNL, spinal nerve ligation; MAP, mean arterial pressure; Cap-SMH, capsaicin induced secondary mechanical hypersensitivity; PWT, paw withdrawal threshold; MPE, maximum possible effect; CFA, complete Freunds' adjuvant; MIA, monoiodoacetic acid; PEG400, polyethlyene glycol 400; FBS, fetal bovine serum; i.v, intraveneous; p.o, per os; PE, phenylephrine.

* Corresponding author at: Abbott Laboratories, R4DE, AP9A-218, 100 Abbott Park Road, Abbott Park, IL 60064-6118, USA. Tel.: +1 847 935 4705; fax: +1 847 937 9195.
E-mail addresses: Victoria.E.Scott@Abbott.com (V.E. Scott), Timothy.Vortherms@Abbott.com (T.A. Vortherms), Wende.Niforatos@Abbott.com (W. Niforatos), Andrew.Swensen@Abbott.com (A.M. Swensen), Torben.Neelands@Abbott.com (T. Neelands), Ivan.Milicic@Abbott.com (I. Milicic), Patricia.Banfor@Abbott.com (P.N. Banfor), Andrew.King@Abbott.com (A. King), Chengmin.Zhong@Abbott.com (C. Zhong), Gricelda.Simler@Abbott.com (G. Simler), CenChen.Zhan@Abbott.com (C. Zhan), Natalie.Bratcher@Abbott.com (N. Bratcher), Janel.Boyce-Rustay@Abbott.com (J.M. Boyce-Rustay), Chang.Zhu@Abbott.com (C.Z. Zhu), Pramila.Bhatia@Abbott.com (P. Bhatia), George.Doherty@Abbott.com (G. Doherty), Helmut.Mack@Abbott.com (H. Mack), Andrew.Stewart@Abbott.com (A.O. Stewart), Michael.Jarvis@Abbott.com (M.F. Jarvis).

0006-2952/$ – see front matter © 2011 Elsevier Inc. All rights reserved.
doi:10.1016/j.bcp.2011.10.019

1. Introduction

Voltage-gated Ca^{2+} channels play an integral role in the regulation of membrane ion conductance and neurotransmission [1]. These channels are classified into low-voltage activated (T-type) and high-voltage activated (L, N, P/Q and R-types) subtypes [2]. Blockade of T- or N-type Ca^{2+} channels leads to antinociception through modulation of neuronal membrane excitability and neurotransmitter release, respectively [3]. N-type Ca^{2+} channels are expressed in pain pathways where they contribute to synaptic transmission between C/Aδ nociceptors and spinal dorsal horn laminae I neurons [4,5]. N-type Ca^{2+} channels in the rostral medial ventral medulla also contribute to descending pain modulation mechanisms [6]. N-type Ca^{2+} channels are composed of a pore forming α_{1B} ($Ca_v2.2$) subunit together with $\alpha_2\delta$ and β subunits that modulate channel expression and kinetic properties. Following nerve injury, the expression levels of $Ca_v2.2$ [7] and $\alpha_2\delta$ [8,9] are elevated in the superficial layers of the dorsal horn of the spinal cord, supporting a role for this channel in neuropathic pain. Additionally, $Ca_v2.2$ knockout mice have reduced nociceptive sensitivity in chronic pain states relative to wild-type controls [10–12]. Pharmacological blockade of N-type Ca^{2+} channels in the CNS by the selective peptide toxin-derived antagonist, ziconotide, effectively attenuates pain responses in rodent preclinical pain models [13–17]. Intrathecal administration of ziconotide (Prialt™) produces symptomatic relief from severe chronic pain in patients for whom opioid therapy is no longer effective [18–20].

A specific role of T-type Ca^{2+} channels in chronic pain states is currently emerging from preclinical studies [21]. T-type Ca^{2+} channels are composed of a single pore forming α subunit and three subtypes exist: $Ca_v3.1$, $Ca_v3.2$ and $Ca_v3.3$ [22]. $Ca_v3.2$ is the predominant T-type Ca^{2+} channel expressed in primary sensory afferent neurons, spinal cord, and brain [23]. Evidence supporting a role of T-type Ca^{2+} channels in neuropathic pain comes from studies that have shown a concurrent increase in the expression of $Ca_v3.2$ channels and after-depolarization potentials in medium diameter Aδ high threshold mechanoreceptor dorsal root ganglion (DRG) neurons in diabetic neuropathic rats [24]. Additionally this increase is also observed in small diameter neurons in the chronic constriction injury of sciatic nerve (CCI) neuropathic pain model in rats [25].

Additional evidence supporting a role of the T-type Ca^{2+} channels in pain comes from gene knockdown studies. Intrathecal $Ca_v3.2$ antisense administration produces a significant knockdown (80–90%) of T-type Ca^{2+} currents in small and medium diameter DRG neurons, and produces robust antihyperalgesic effects in the CCI model of neuropathic pain in rats [26]. Moreover, $Ca_v3.2$ knockout mice show decreased pain responses compared to wild-type mice in acute mechanical, thermal, and chemical pain models [27].

It has been proposed that voltage-dependent Ca^{2+} channel blockers, that preferentially bind to and stabilize inactivated states of the channel, may produce robust antinociception without producing deleterious effects of cardiovascular or CNS function, which have been associated with the voltage-independent peptide blocker ziconotide [28–30]. This state-dependent ion channel blocker hypothesis has been demonstrated clinically for other voltage-gated channels including Na^+ channel blockers and for L-type Ca^{2+} channel blockers [31–33]. In the present study two structurally novel Ca^{2+} channel blockers A-686085 and A-1048400 (Fig. 1) that have similar activities at neuronal N- and T-type Ca^{2+} channels, but differ in their activity at L-type Ca^{2+} channels were evaluated for their ability to produce antinociception and alter hemodynamic function in the rat. The ability of the diphenylpiperazine chemotype to block voltage-gated Ca^{2+} channels has been well documented [3,29,34]. The diphenyl lactam variants represented by A-686085 and A-1048400 are structurally novel and offer new opportunities to develop structure activity relationships for this general pharmacophore (Doherty et al., submitted for publication).

2. Materials and methods

2.1. N-type Ca^{2+} flux fluorometric imaging plate reader based assay

A Ca^{2+} flux Fluorometric imaging plate reader (FLIPR) based assay that was previously described [35,36] was utilized to identify novel N-type Ca^{2+} channel blockers. All reagents used in these studies were from Sigma–Aldrich (St. Louis, MO) unless otherwise stated. IMR32 human neuroblastoma cells (ATCC CCL-127) were maintained in Minimum Essential Media (MEM) containing 10% FBS (fetal bovine serum), 1% antibiotic/antimycotic, 1% sodium pyruvate, and 1% MEM non-essential amino acids (Invitrogen, Carlsbad, CA, USA) and incubated at 37 °C with 5% CO_2. Following thorough washing with Ca^{2+}- and Mg^{2+}-free PBS (Invitrogen, Carlsbad, CA), cells were removed from the tissue culture flask by triturating with growth media, resuspended and seeded at a density of 1.2×10^5 cells per well in black 96-well CellBIND (Corning, Lowell, MA) coated plates. Cells were incubated for 48 h at 37 °C in a humidified incubator with 5% CO_2 prior to use in the Ca^{2+} flux assay. Calcium 4 dye (R7446; Molecular Devices, Sunnyvale, CA) was prepared as a 10× stock solution by diluting one vial with 10 ml Hank's Balanced Salt Solution (HBSS) containing 20 mM HEPES, pH 7.4 (Invitrogen, Carlsbad, CA) and was stored in the dark at −20 °C. On the day of the experiment, the 10× stock Calcium 4 dye was diluted 1:20 with HBSS containing 20 mM HEPES, pH 7.4. The growth medium was removed and the cells were then incubated with 100 μl of diluted Calcium 4 dye for 1.5 h at room temperature in presence of 2 μM nifedipine (final concentration; [36]) to block endogenous L-type Ca^{2+} channels that are also expressed in IMR32 cells. A-1048400 (MW = 543) and A-686085 (MW = 572) were synthesized at Abbott Laboratories (Abbott Park, IL), prepared as 10 mM stock solutions in dimethyl sulfoxide (DMSO) and diluted to 4X final concentrations ranging from 30 μM to 1 nM using Ca^{2+}- and Mg^{2+}-free HBSS. The maximum DMSO concentration in the assay was 0.3%. A-1048400 and A-686085 (50 μl) were pre-incubated with the cells during dye loading for 1 h. The channels were activated by addition of 50 μl of a high concentration of KCl and $CaCl_2$ prepared to 4× final concentration of 80 and 5 mM, respectively in Ca^{2+}- and Mg^{2+}-free HBSS containing 20 mM HEPES, pH 7.4. Background fluorescence was measured using Ca^{2+}- and Mg^{2+}-free HBSS in the absence of the KCl. Data are plotted as the percent of control response in the absence of antagonist and IC_{50} values were determined following nonlinear regression analysis using the Levenberg–Marquardt curve fitting algorithm in GraphPad Prism (La Jolla, CA).

2.2. T-type Ca^{2+} flux FLIPR based assay

A FLIPR based Ca^{2+} flux assay previously described [37] was utilized to characterize the ability of compounds to block T-type Ca^{2+} channel activity. Recombinant human $Ca_v3.2$ stably expressed in HEK293 cells was provided by Dr. Ed Perez-Reyes (University of Virginia, VA) and maintained in high glucose Dulbecco's Modified Eagle's Medium (DMEM) containing 10% FBS and 1 mg/ml G418 (Invitrogen, Carlsbad, CA). Following gentle trypsinization for 1–2 min using 0.25% trypsin-EDTA (Invitrogen, Carlsbad, CA), cells were resuspended in growth medium and seeded at a density of 6.0×10^4 cells per well in black walled 96-well poly-D-Lysine coated plates (Corning, Lowell, MA). Cells were incubated for 24 h at 37 °C in a humidified incubator with 5% CO_2

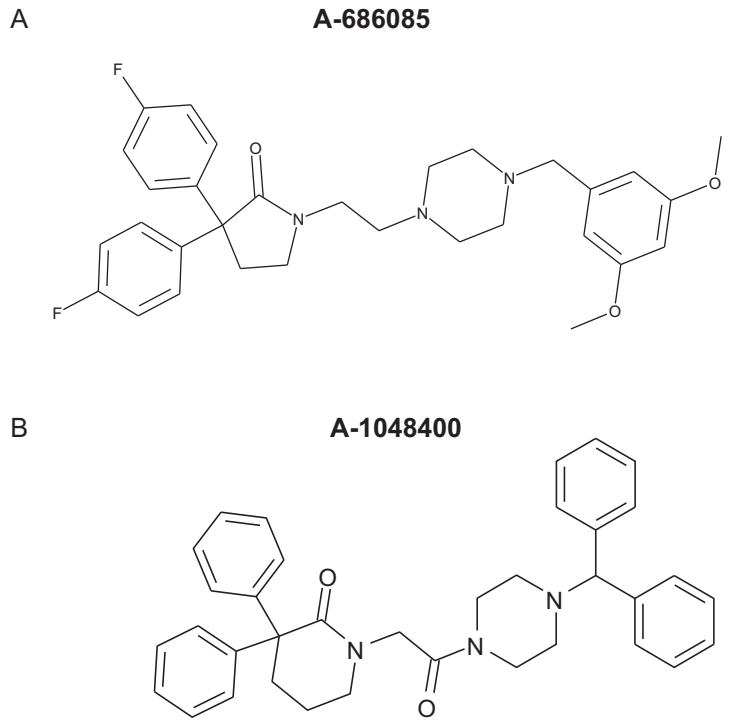

Fig. 1. The chemical structures of (A) A-686085 (1-(2-(4-(3,5-dimethoxybenzyl)piperazin-1-yl)ethyl)-3,3-bis(4-fluorophenyl)pyrrolidin-2-one) and (B) A-1048400 (1-[2-(4-benzhydryl-piperazin-1-yl)-2-oxo-ethyl]-3,3-diphenyl-piperidin-2-one) are shown.

prior to use in the Ca^{2+} flux assay. Calcium blue dye (R7265; Molecular Devices, Sunnyvale, CA) was prepared as a 10× stock solution by diluting one vial with 10 ml HBSS, containing 20 mM HEPES, pH 7.4. This 10× stock calcium dye was diluted 1:10 with Ca^{2+}- and Mg^{2+}-free HBSS containing 20 mM HEPES, pH 7.4. The growth medium was removed using gently aspiration and the cells were then incubated with 100 μl of diluted calcium blue dye for 2–3 h at room temperature. A-1048400 and A-686085 were prepared as a 10 mM stock solution in DMSO. The maximum DMSO concentration was 0.3%. A-1048400 and A-686085 (50 μl) were pre-incubated with the cells for 3 min at room temperature. Activation of $Ca_v3.2$ was achieved by addition of a $CaCl_2$ trigger (50 μl of 5 mM $CaCl_2$ (final concentration) prepared in Ca^{2+}- and Mg^{2+}-free HBSS containing 20 mM HEPES, pH 7.4). Background fluorescence was measured using Ca^{2+}- and Mg^{2+}-free HBSS in the absence of the $CaCl_2$ trigger. Data are plotted as the percent of control response in the absence of antagonist and IC_{50} values were determined following nonlinear regression analysis using the Levenberg–Marquardt curve fitting algorithm in GraphPad Prism (San Diego, CA).

2.3. Rat aorta ring tissue relaxation assay

Male Sprague–Dawley rats (200–350 g; Charles River Laboratories, Wilmington, MA) were euthanized with CO_2 and decapitated. The entire thoracic aorta was removed and immediately placed into Krebs Ringer bicarbonate solution and equilibrated with 5% CO_2; 95% O_2. The pH was adjusted to 7.2 at 25 °C by titrating with a saturated solution of $NaHCO_3$. The pH increased to 7.4 at 37 °C. Propranolol (Sigma–Aldrich, 0.004 mM was included in all of the assays to block β adrenoreceptors [38]. The aorta was cleaned of extraneous tissue and the endothelium removed by passing a 100 mm length of PE-160 tubing through the lumen. The aorta was cut into 3–4 mm rings and mounted in 10 ml isolated tissue baths at 37 °C. The aorta from each rat supplied 8 tissue rings with one end of the aorta fixed to a stationary glass rod and the other to a Grass FT03 transducer at a basal preload of 1.0 g. Tissues were rinsed every 10 min for a total of 45–60 min. The aorta was primed once with 80 mM KCl, rinsed and allowed to return to basal tension and again with 10 μM phenylephrine (PE). Absence of functional endothelium was confirmed by loss of the acetylcholine-induced (10 μM) relaxation performed at the end of the PE prime step. After an additional 30 min equilibration period tension was established using 80 mM KCl solution (200 μl of 4.0 M stock solution). A relaxation concentration response curve was generated for each tissue. Data collection was by Power-Lab/800 data acquisition system (Castle Hill, Australia). A cumulative concentration protocol was employed and each tissue was used once. The amount of A-1048400 or A-686085 necessary to cause a 50% reversal (ED_{50}) of 80 mM KCl evoked contraction was calculated by nonlinear regression analysis using the Levenberg–Marquardt curve fitting algorithm in GraphPad Prism.

2.4. Electrophysiological assessment of N, T and P/Q-type Ca^{2+} channels in HEK293 cells

The activity of A-1048400 at N-type ($Ca_v2.2$, $\alpha_2\delta_1/\beta_{1b}$), T-type ($Ca_v3.2$) and P/Q-type ($Ca_v2.1/\alpha_2\delta_1/\beta_{1b}$) calcium channels over-expressed in HEK293 cells was determined using manual whole cell patch clamp techniques. The N-type cell line was provided by Dr. Diane Lipscombe (Brown University, Providence, RI). The N- and T-type Ca^{2+} channel cell lines used in these studies were previously characterized [37,39]. For the P/Q type cell line human $Ca_v2.1$ (Reference Sequence No. NM_000068), $\alpha_2\delta$ (Reference Sequence No. NM_000722) and β_{1b} (Reference Sequence No. NM_000723) were amplified from cDNA generated from human brain total RNA by RT-PCR. The full length cDNA fragment for $Ca_v2.1$ was subcloned into the mammalian expression vector pcDNA 3.1 – Hygromycin (Invitrogen, Carlsbad, CA). The cDNA encoding the $\alpha_2\delta$ and β_{1b} subunits were subcloned into the dual mammalian expression vector pBUDCE4.1 – zeocin (Invitrogen,

Carlsbad, CA). The human $Ca_v2.1$ and $Ca_v \alpha_2\delta/Ca_v \beta_{1b}$ expression vectors were co-transfected into human HEK293 by electroporation using the time constant mode of 800 V for 0.2 ms in the Gene Pulsar 2 electroporator (Biorad, Hercules, CA). Single colonies surviving selection by hygromycin (100 μg/ml) and zeocin (100 μg/ml) (Invitrogen, Carlsbad, CA) were screened for functional P/Q-type Ca^{2+} channel activity by whole cell patch-clamp recordings (see below) and were propagated as stable cell lines. Cells were maintained in high glucose-containing DMEM, containing 10% FBS and hygromycin (100 μg/ml) and zeocin (100 μg/ml) to maintain selection pressure.

To assess functional activity of the channels by electrophysiology, cells expressing each Ca^{2+} channel subtype were continuously superfused by an extracellular recording solution at room temperature consisting of (mM): 5 $BaCl_2$ (N- and P/Q-type) or 5 $CaCl_2$ (T-type), 87.5 CsCl, 40 TEA-Cl, 1 $MgCl_2$, 10 HEPES, and 10 glucose. The pH was adjusted to 7.2 with CsOH and the osmolarity was adjusted to approximately 310 mOsM with sucrose. Intracellular solutions for N-, T-and P/Q-type experiments consisted of (mM): 56 CsCl, 68 CsF, 2.2 $MgCl_2$, 4.5 EGTA, 9 HEPES, 4 Mg_2ATP, 14 Creatine phosphate, and 0.3 GTP. The pH was adjusted to 7.4 with CsOH with an osmolarity of approximately 290 mOsM. For the T-type channel studies, cells were held at a membrane potential of −120 mV (closed state) or −70 to −75 mV (inactivated state) prior to a 100 ms test pulse to −30 mV at a frequency of 0.2 Hz. For N-type and P/Q-type Ca^{2+} channels, the cells were held at a membrane potential of −120 mV (closed state), −80 to −90 mV (P/Q-type inactivated state), or −80 mV (N-type inactivated state) with a 50 ms step to +10 mV at a frequency of 0.2 Hz. A-1048400 was tested from a low to high concentration reaching a plateau with each dose tested (approximately 3–5 min).

2.5. Assessment of native N-type and T-type Ca^{2+} channels in rat DRG neurons by electrophysiology

DRG neurons were isolated from adult Sprague–Dawley rats (250–300 g) that were CO_2-euthanized and decapitated, and their vertebral columns removed. DRG neurons were dissected from the lumbar level of the vertebral column and placed in DMEM containing 0.3% collagenase B/collagenase-dispase (Roche, Indianapolis, IN) for approximately 90 min at 37 °C and 5% CO_2. After washing in fresh DMEM, ganglia were dissociated by trituration using a sterile fire-polished Pasteur pipette to obtain a single-cell suspension. DRG neurons were then plated on polyethelenimine-treated 12 mm glass coverslips at a density of one DRG per coverslip in 1 ml DMEM supplemented with 10% FBS, NGF (50 ng/ml) and 100 IU/ml penicillin/streptomycin (Invitrogen, Carlsbad, CA). Neurons were used for electrophysiological recording within 2–24 h after plating.

For whole-cell voltage-clamp experiments, recording solutions were identical to those described above for the stably transfected $Ca_v3.2$ HEK cells. To assess inhibition of T-type calcium currents, DRG neurons were voltage-clamped at −70 to −75 mV and stepped to −30 mV at a frequency of 0.2 Hz. Voltage steps to −30 mV were used so that T-type currents could be elicited with minimal contamination from high threshold calcium currents [40]. The currents elicited with the steps to −30 mV exhibited kinetics characteristic of T-type calcium currents. DRG neurons with diameters of 35–42 μm were selected because of their higher expression of T-type currents [41].

To assess inhibition of N-type current, DRG neurons were voltage clamped at −60 to −65 mV and stepped to 0 mV at a frequency of 0.2 Hz. The step to 0 mV was preceded by a 200 ms step to −30 mV to inactivate T-type calcium channels. To minimize the contribution from non-N-type high-threshold calcium channels, 1 μM nifedipine, 150 nM SNX-482 (Peptides International Inc, Louisville, KY), and 300 nM ω-Aga-IVA were included in the external solution to block L-type [42], R-type [43], and P/Q-type [44] currents, respectively. For N-type recordings, the rat DRG neurons were between 25 and 35 μm in diameter.

For determining compound 50% inhibition concentration (IC_{50}) values for manual electrophysiology, averaged percent control values were plotted as a function of compound concentration and fitted using a four parameter logistic equation with the minimum fixed at zero and maximum fixed to 100% of control. For the fit of the P/Q-type data a shared hill slope was used since there were only two points defining the slope between 10% and 90% for the hyperpolarized holding potential.

2.6. Ancillary pharmacology

A-1048400 was profiled against a large panel of *in vitro* binding assays (CEREP, Poitiers, France) as previously described [45]. These binding assays included the following receptors, ion channels and enzymes: Adenosine A1, Adenosine A2A, Adenosine A3, Adrenergic α_1, Adrenergic α_2, Adrenergic β_1, Adrenergic β_2, Angiotensin AT1, Angiotensin AT2, Benzodiazepine Central, Benzodiazepine Peripheral, Bombesin, Bradykinin B2, CGRP, Cannabinoid CB1, CCKA, CCKB, Dopamine D1, Dopamine D2, Dopamine D3, Dopamine D4.4, Dopamine D5, Endothelin ETA, Endothelin ETB, GABA, Galanin GAL1, Galanin GAL2, PDGF, TNFa, CCR1, Histamine H1, Histamine H2, MC4, MT1, Muscarinic M1, Muscarinic M2, Muscarinic M3, Muscarinic M4, Muscarinic M5, Neurokinin NK1, Neurokinin NK2, Neurokinin NK3, Neuropeptide Y1, Neuropeptide Y2, Neurotensin NT1, Opioid d2, Opioid m, Opioid k, ORL1, PACAP (PAC1), EP4, TP, IP, P2X, P2Y, Serotonin 5-HT1A, Serotonin 5-HT1B, Serotonin 5-HT2A, Serotonin 5-HT2C, Serotonin 5-HT3, Serotonin 5-HT5A, Serotonin 5-HT6, Serotonin 5-HT7, Somatostatin receptor, glucocorticoid receptor, VIP1 (VPAC1), Vasopressin V1a, Ca^{2+} channel verapamil site, K^+channel (Voltage dependent), K^+ Channel (Ca^{2+} dependent), Cl^- Channel, Norepinephrine transporter, Dopamine transporter, 5-HT-transporter.

Compounds that showed >50% activity in binding assays were evaluated for effects in functional assays at CEREP or at Abbott Laboratories.

2.7. Pharmacokinetic analysis

The pharmacokinetic properties were determined in Sprague–Dawley rats dosed with 3 μmol/kg A-1048400 or A-686085 prepared in 10% DMSO/90% poly ethylene glycol 400 (PEG400). The plasma levels of A-1048400 and A-686085 were determined using HPLC and mass spectrometry. Results from preliminary characterization of the pharmacokinetic profiles of these compounds indicated that plasma levels following oral (p.o.) administration of A-1048400 at 30 mg/kg was 0.37 μg/ml after 60 min and intraperitoneal (i.p.) administration of A-686085 at 3 mg/kg after 30 min was 0.30 μg/ml. Consequently, p.o. and i.p. routes of administration were used for the pain behavior studies of A-1048400 and A-686085, respectively. Following oral administration of the A-1048400 (3, 10 and 30 mg/kg) prepared in 10% PEG400/10% Cremophor EL/80% Oleic Acid the levels of A-1048400 in plasma and brain were determined. Briefly, the brains were immediately removed and freed from blood vessels as much as possible. The resulting brain tissues were frozen at −20 °C, followed by weighing and homogenization before analysis. The heparinized blood samples were frozen (−20 °C) until analysis. A-1048400 was separated from the blood and brain samples using protein precipitation with acetonitrile followed by quantification with liquid chromatography/mass spectroscopy. The brain to plasma ratio was determined to be 1:10 (data not shown). Brain levels for A-686085 were not determined.

2.8. Anesthetized rat cardiovascular studies

The effects of A-1048400 and A-686085 on hemodynamic and cardiovascular function in the anesthetized rat were performed as described previously [46]. Briefly, male Sprague–Dawley rats (325–400 g) were anesthetized with the long-acting barbiturate inactin (100 mg/kg, i.p.). Catheters were inserted into the femoral artery, to allow measurements of arterial pressure and heart rate, and also into the femoral vein for drug infusion. In addition, a Millar micro tip transducer was inserted into the left ventricle via the right carotid artery to measure left ventricular pressure and provide an index of left ventricular contractility (dP/dt_{50}). Following a 30 min baseline period, A-1048400 or A-686085 was infused intravenously at 3, 10, and 30 mg/kg/30 min or 0.3, 1.0 and 3.0 mg/kg/30 min, respectively, prepared in PEG400 (1 ml/kg). The effects on mean arterial pressure (MAP), heart rate and left ventricular contractility (dP/dt_{50}), were assessed by a computerized data acquisition program (Ponemah 4.8, Data Sciences International, St. Paul, MN) and reported as a percentage of vehicle control. To determine the exposure levels of A-1048400 in plasma, blood samples were taken at the end of each 30 min infusion period and plasma levels were quantified by HPLC and mass spectrometry.

2.9. Behavior studies

In all behavioral studies, male Sprague–Dawley rats (200–350 g) were used. Animals were housed five per cage, and in quarantine for 5–7 days before entering the study. All animals were kept in a temperature-regulated environment under a controlled 12-h light–dark cycle with lights on at 6:00 A.M. Food and water were provided *ad libitum*. All procedures were performed in an Association for Assessment and Accreditation of Laboratory Animals Care (AAALAC) approved facility and approved by the Institutional Animals Care and Use Committee (IACUC) at Abbott Laboratories and conducted in accordance with the ethical principles for pain-related animal research of the American Pain Society. For behavioral testing, A-1048400 or A-686085 was either orally (p.o.) or i.p. administered, prepared in 10% PEG400/10% cremophor EL/80% oleic acid in a volume of 2 ml/kg. Haloperidol or MK-801 was p.o. administered, prepared in water 2.0 ml/kg

2.9.1. Capsaicin-induced secondary mechanical hypersensitivity

A model of capsaicin-induced secondary mechanical hypersensitivity (Cap-SMH) in rats was produced as previously described [47]. Following a 30 min acclimation to the testing room, 10 μg capsaicin in a 10 μl solution of 10% ethanol/90% hydroxypropyl-β-cyclodextrin was injected subcutaneously in the ventral aspect of the right hind paw of the rats. A-1048400 was p.o. administered at 3, 10, 30 and 100 mg/kg 2 h following capsaicin-injection, and mechanical allodynia was assessed 60 min after compound treatment (3 h after capsaicin-injection). A-686085 was i.p. administered at 3, 10, 30 and 100 mg/kg 150 min following capsaicin-injection, and mechanical allodynia was assessed 30 min after compound treatment (3 h after capsaicin-injection). Mechanical allodynia was assessed in the ipsilateral capsaicin-injected paw. Rats were placed into inverted individual plastic containers (20 cm × 12.5 cm × 20 cm) on top of a suspended wire mesh with a one cm^2 grid to provide access to the ventral side of the hind paws, and acclimated to the test chambers for 20 min. Testing was performed with von Frey monofilaments (Stoelting, Wood Dale, IL) applied at the heel away from the site of capsaicin injection. Paw withdrawal threshold (PWT) was determined by increasing and decreasing stimulus intensity, and estimated using the Dixon's up-down method [48]. The von Frey filaments were presented perpendicularly to the plantar surface of the selected hind paw, and then held in this position for approximately 8 s with enough force to cause a slight bend in the filament. Positive responses included an abrupt withdrawal of the hind paw from the stimulus, or flinching behavior immediately following removal of the stimulus. A 50% withdrawal threshold was determined using an up-down procedure [49]. The strength of the maximum filament used for von Frey testing was 15.0 gram (g). A percent maximal possible effect (% MPE) of testing compound was calculated following the formula: (log[compound-treated threshold] − log[-log[vehicle-treated threshold])/(log[maximum threshold] − log [vehicle-treated threshold]) × 100%, where the maximum threshold was equal to 15.0 g.

2.9.2. Monoiodoacetic acid (MIA) induced knee joint pain model

Studies using this model were performed as previously described [50]. Briefly, unilateral knee joint osteoarthritis was induced in the rats by a single intra-articular injection of MIA (3 mg in 50 μl sterile isotonic saline) into the joint cavity using a 26 G needle under light (2–4%) halothane (Halocarbon Laboratories, River Edge, NJ) anesthesia. Following injection, the animals were allowed to recover from the anesthesia (usually 5–10 min) before returning them to their home cages. At least 21 days post MIA-injection, A-1048400 was p.o. administered at 3, 10 and 30 mg/kg, and grip force strength was assessed 60 min following compound treatment. Measurements of hind limb grip force were conducted by recording the maximum compressive force (CF_{max}) exerted on the hind limb strain gauge, in a commercially available grip force measurement system (Columbus Instruments, Columbus, OH). During testing, each rat was gently restrained and allowed to grasp the wire mesh frame attached to the strain gauge. The experimenter then moved the animal in a rostral-to-caudal direction until the grip was broken. Each rat was sequentially tested twice at an approximately 2–3 min interval to obtain a raw mean compressive grip force (CF_{max} in gram force units) [50]. In order to account for the body weight differences among the rats, this raw mean grip force was converted to a maximum hind limb compressive force for each animal by dividing the CF_{max} by the body weight of the rat in kg [(CF_{max} in gram force)/kg body weight]. A group of age matched naïve animals was included in each experiment. The data obtained from various dose groups for the test compound were compared with data from the naïve group. The vehicle control group was assigned a value of 0% whereas the naïve group was assigned a value of 100%. The % effects for each dose-group were expressed as % return to normal grip force as found in the naïve group, and calculated using the formula: (% return to normalcy = [(treatment CF_{max} − vehicle CF_{max})/(Naïve CF_{max} − vehicle CF_{max})] × 100%).

2.9.3. Complete Freunds' adjuvant (CFA)-induced mechanical allodynia

Mechanical allodynia was induced by injection of 150 μl of a 50% solution of CFA in phosphate buffered saline into the plantar surface of the right hind paw in rats. Forty-eight hours following CFA injection, A-1048400 was p.o. administered at 3, 10, 30 and 100 mg/kg, and mechanical allodynia of CFA-injected paw was assessed 60 min after compound administration. Percentage MPE was calculated as described above for Cap-SMH.

2.9.4. Spinal nerve ligation (SNL)

Rats received unilateral ligation of the lumber 5 (L5) and lumbar 6 (L6) spinal nerves as previously described [51]. The left L5 and L6 spinal nerves of the rat were isolated adjacent to the vertebral column and tightly ligated with a 5–0 silk suture distal to the DRG, and care was taken to avoid injury of the L4 spinal nerve. All animals were allowed to recover for at least 1 week and not more than 3 weeks prior to assessment of mechanical allodynia. PWT

was assessed in these animals as described above for Cap-SMH rats. Only rats with a PWT ≤4.5 g were considered allodynic and utilized to test the analgesic activity. A-1048400 was p.o. administered at 3, 10 and 30 mg/kg, and mechanical allodynia was assessed 60 min after compound administration. Percentage MPE was calculated as described above for Cap-SMH.

2.9.5. Chronic constriction injury of the sciatic nerve

A model of chronic constriction injury-induced neuropathic pain in rats was produced by following the method of Bennett and Xie [52]. The right common sciatic nerve was isolated at mid-thigh level, and loosely ligated by 4 chromic gut (5–0) ties separated by an interval of 1 mm. All animals were left to recover for at least 2 weeks and no more than 4 weeks prior to testing of mechanical allodynia. PWT was assessed in these animals as described above for Cap-SMH, Only rats with a PWT ≤4.5 g were considered allodynic and utilized to test the analgesic activity. A-1048400 was p.o. administered at 10, 30 and 100 mg/kg, and mechanical allodynia was assessed 60 min after compound administration. Percentage MPE was expressed as described above for Cap-SMH.

2.9.6. Rotarod performance

Rotarod performance was measured using an accelerating Rotarod apparatus (Omnitech Electronics, Inc. Columbus, OH). Rats were acclimated for period of 30 min in the testing room. Each rat was then given three training sessions by being placed on a 9 cm diameter rod that increased in speed from 0 to 20 rpm over a 60 s period. The time required for the rat to fall from the rod was recorded with a maximum score of 60 s. A-1048400 was p.o. administered at 30, 100 and 300 mg/kg, with haloperidol administered at 3.7 mg/kg, p.o. as a positive control. The rats were placed back on the Rotarod apparatus for 3 consecutive testing trials 60 min after compound administration. Compounds that impair motor-coordination in this model yield shorter latency to fall.

2.9.7. Modified edge test

Using an edge-balance assay developed in our laboratory, rats were acclimated to the test room for 30 min, and were then placed on the edge (0.25 inch wide) of the rectangular Plexiglas box (40 cm × 40 cm × 38 cm), the time to fall off the top of the vertical wall was determined and reported as fall latency, with a maximum cut-off point of 120 s [53]. A-1048400 was p.o. administered at 30, 100 and 300 mg/kg, with MK-801 administered at 0.1 mg/kg, p.o. as positive control, and edge performance was assessed 60 min after compound administration.

2.9.8. Statistics

Analysis of the *in vivo* data was carried out using one way analysis of variance (one-way ANOVA). Where appropriate, Bonferroni multiple comparison test was used for post hoc analysis (GraphPad Prism). The level of significance was set at $p < 0.05$. Data are presented as mean ± SEM. ED_{50} values and the 95% confidence intervals (95% CI) were estimated from the prism graph. Experimenters were blinded to drug treatment.

3. Results

3.1. Identification of two structurally novel neuronal Ca^{2+} channel blockers

The IMR32 human neuroblastoma cell line expresses both N- and L-type channels [54]. To selectively assess N-type channel activity in the IMR32 cells 2 μM nifedipine was included to block activation of the endogenous L-type Ca^{2+} channels in these cells. A-686085 (Fig. 1) was identified following screening of the Abbott compound collection as a potent (IC_{50} = 0.8 μM (95% CI: 0.4–1.8 μM; Fig. 2A)) N-type Ca^{2+} channel blocker using this IMR32 FLIPR assay. A-686085 also blocked T-type Ca^{2+} channels with an IC_{50} = 4.6 μM (95% CI: 4.5–4.7 μM) (data not shown) determined at the human $Ca_v3.2$ channel stably expressed in HEK293 cells using a FLIPR based Ca^{2+} flux assay [37]. In addition to its activity at N-type and T-type Ca^{2+} channels, A-686085 was also active in a rat aorta tissue relaxation assay (EC_{50} = 0.6 μM (95% CI: 0.5–0.6 μM; Fig. 2B), a preparation used to detect functional block of native L-type Ca^{2+} channels [55].

Structure activity relationship (SAR) studies based on A-686085 led to the discovery of A-1048400 (Doherty et al., submitted for publication; Fig. 1). A-1048400 potently inhibited N-type (IC_{50} = 1.4 μM (95% CI: 1.1–1.7 μM; Fig. 2A) and T-type Ca^{2+} channels (IC_{50} = 1.2 μM (95% CI: 1.1–1.4) (data not shown). In contrast to A-686085, A-1048400 was significantly less active in rat aorta tissue relaxation assay (EC_{50} = 28 μM (95% CI: 22.8–35.7 μM; Fig. 2B. The effect of the test compound vehicle (DMSO, 0.6%) was not significant in this assay. For comparison, nifedipine potently relaxed pre-contracted rat aorta rings with an EC_{50} = 12.6 nM (95% CI: 10.8–14.8 nM). The N-type Ca^{2+} channel selective peptide blocker ω-conotoxin GVIA did not relax pre-contracted smooth muscle rings at concentrations up to 3 μM (Fig. 2B). These data suggest that A-1048400 has approximately 20-fold greater activity in blocking N-type Ca^{2+} channels compared to L-type Ca^{2+} channels assessed using the rat aorta tissue relaxation assay. A-686085, in contrast, has equivalent activity at both N-type and L-type Ca^{2+} channels.

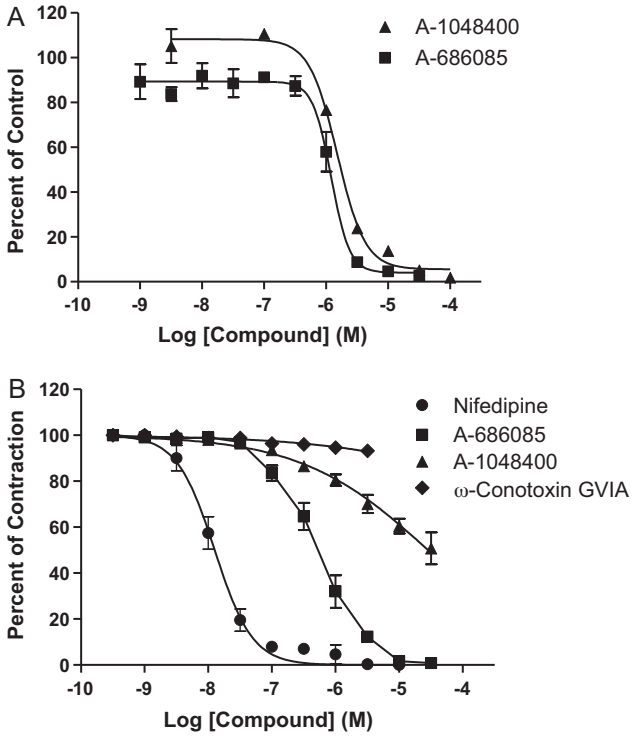

Fig. 2. (A) The ability of A-1048400 (▲) and A-686085 (■) to dose-dependently (1 nM to 100 μM) inhibit KCl-evoked Ca^{2+} influx at N-type Ca^{2+} channels endogenously expressing in IMR32 cells was assessed in a FLIPR based Ca^{2+} flux assay. Data are presented as a percent of control response ± SEM in the absence of test compound (n = 3). (B) The ability of A-1048400 (▲) and A-686085 (■) to dose-dependently relax KCl evoked contractions in rat aorta was assessed. The selective L-type blocker nifedipine (●) and the N-type selective blocker ω-conotoxin GVIA (◆) were included as positive and negative controls, respectively. The rat aorta was pre-contracted to 1 g tension with 80 mM KCl and the ability of test compounds to relax the tissue was measured following cumulative additions of each blocker over 15 min intervals. The data is presented as % of contraction (n = 3).

3.2. Effects of A-686085 and A-1048400 on Cap-SMH

A-686085 dose dependently attenuated capsaicin-induced secondary mechanical hypersensitivity, with an estimated ED_{50} of 3 mg/kg i.p. (95% CI: 2.7–5.2 mg/kg; Fig. 3A; $n = 6$ per group), corresponding to plasma concentration of 0.30 μg/ml. Similarly, A-1048400 dose dependently attenuated mechanical hypersensitivity, with an estimated ED_{50} = 28 mg/kg p.o. (95% CI: 17–66 mg/kg; Fig. 3B; $n = 12$ per group) and a corresponding plasma concentration of 0.37 μg/ml at 30 mg/kg.

3.3. Differential effects of A-686085 and A-1048400 on rat hemodynamics

To assess the hemodynamic effects of A-1048400 and A-686085, the ability of these compounds to alter MAP, heart rate, and left ventricular contractility (dP/dt_{50}) was evaluated in an anesthetized rat cardiovascular assay [46]. A-686085 was intravenously (i.v.) administered in ascending doses of 0.3, 1.0 and 3.0 mg/kg over a 30 min infusion period. This infusion protocol generated plasma concentrations of 0.1, 0.3 and 0.7 μg/ml, respectively (Table 1). A-686085 significantly reduced MAP at plasma concentrations as low as 0.1 μg/ml (Table 1), and MAP was markedly reduced to 58% at 0.7 μg/ml relative to vehicle-treated rats. A-686085 had no significant effects on heart rate but there was a slight increase in left ventricular contractility (dP/dt_{50}) at all doses (Table 1). A-1048400 was administered i.v. in ascending doses of 3, 10 and 30 mg/kg over a 30 min infusion period. This infusion protocol generated plasma concentrations at the end of each dose of 1.0, 4.9 and 11.9 μg/ml, respectively (Table 1). A-1048400 produced no significant effects on MAP, heart rate and left ventricular contractility (dP/dt_{50}) at plasma concentrations up to 4.9 μg/ml (Table 1), although at the highest plasma concentration tested (11.9 μg/ml) A-1048400 produced a modest but not significant decrease in heart rate (Table 1).

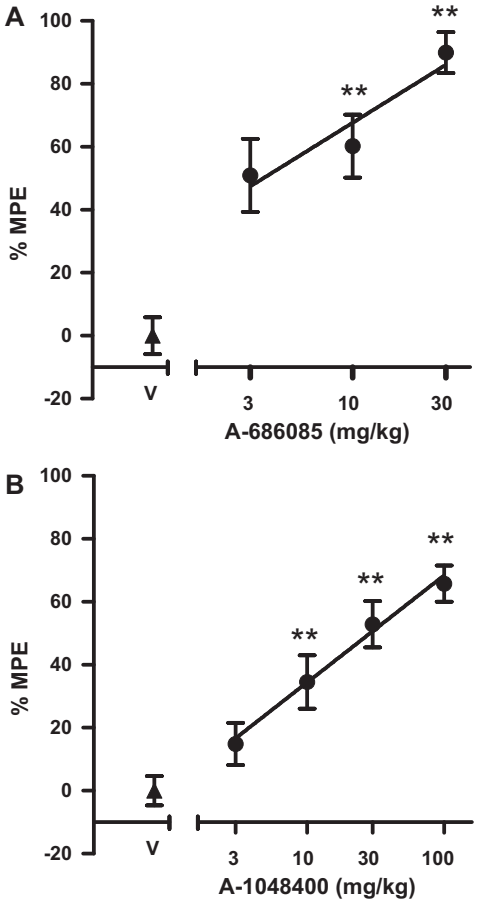

Fig. 3. Effects of A-686085 and A-1048400 on Cap-SMH in rats. (A) A-686085 was administered i.p. at 3, 10 and 100 mg/kg 150 min following capsaicin-injection, and mechanical allodynia was assessed 30 min after compound treatment (3 h after capsaicin-injection). (B) A-1048400 was administered orally at 3, 10 and 100 mg/kg 2 h following capsaicin-injection, and mechanical allodynia was assessed 60 min after compound treatment (3 h after capsaicin-injection) (A). Data (●) are expressed as the percentage of maximal possible effect (% MPE) ± SEM, $^{**}p < 0.01$ vs. vehicle-treated rats ($n = 12$ per group). Data is also shown for vehicle (▲) treated rats. V: vehicle.

The cardiovascular profile for A-686085 is similar to the hemodynamic effects of L-type Ca^{2+} channel blockers such as nifedipine [56] and is likely to be due to the ability of A-686085 to block L-type channels. Taken together, these data demonstrate that A-1048400 has at least a 14-fold margin for reducing nociception in the Cap-SMH model compared to its ability to reduce hemodynamic function in the rat. In contrast, A-686085 was approximately 3-fold more potent in reducing hemodynamic function compared to its antinociceptive activity in the Cap-SMH model.

Since A-1048400 was shown to have selective antinociceptive activity at plasma concentrations that did not significantly alter hemodynamic function, additional *in vitro* and *in vivo* studies were carried out to further characterize the pharmacology of this novel neuronal Ca^{2+}channel blocker.

3.4. Electrophysiological characterization of A-1048400 at voltage-dependent Ca^{2+}channels

The ability of A-1048400 to block N-type Ca^{2+} channels was confirmed using whole-cell patch clamp recordings in HEK293 cells that stably expressed N-type Ca^{2+}channels [39]. To assess whether or not A-1048400 inhibition was state-dependent, channel block was measured under both hyperpolarized conditions, where channels are predominantly in the closed state, and more depolarized conditions, where channels are biased towards inactivated states. From a hyperpolarized holding potential of −120 mV, A-1048400 blocked N-type calcium current with an IC_{50} = 4.1 μM (95% CI: 2.8–6.1 μM; Fig. 4A; Table 2). From a more depolarized, inactivating holding potential of −80 mV, the IC_{50} value was reduced to 0.8 μM (95% CI: 0.7–1.0 μM; Fig. 4A; Table 2). This represents a five-fold shift in potency and suggests a state-dependent mechanism of inhibition for A-1048400.

Additional studies were performed using stably expressed recombinant human Ca^{2+} channels in HEK293 cells by whole-cell patch clamp recordings. At a holding potential of −110 mV, A-1048400 blocked the T-type ($Ca_v3.2$) Ca^{2+} current with an IC_{50} = 2.6 μM (95% CI: 2.0–3.4 μM; Fig. 4B; Table 2) while at holding potentials of −70 to −75 mV where the channels are biased towards the inactivated state, A-1048400 blocked the T-type Ca^{2+} current with an IC_{50} = 0.9 μM (95% CI: 0.8–1.0 μM; Fig. 4B; Table 2). A-1048400 also blocked P/Q-type Ca^{2+} channels. At a holding potential of −120 mV, A-1048400 blocked P/Q-type Ca^{2+} current with an IC_{50} = 16.1 μM (95% CI: 4.7–56 μM; Fig. 4C) and at a holding potential of −90 mV the current was blocked with an IC_{50} = 1.3 μM (95% CI: 0.5–3.4 μM; Fig. 4C; Table 2). These data suggest that A-1048400 is a voltage-dependent Ca^{2+} channel blocker that has preferential affinity for the inactivated state of N-, T- and P/Q-type Ca^{2+} channels.

3.5. A-1048400 blocks native N-type and T-type Ca^{2+} channels expressed in DRG neurons

In electrophysiological studies using acutely dissociated rat DRG neurons that were held at a membrane potential of

Table 1
The cardiovascular effects of A-686085 and A-1048400 in anesthetized rat.

Cardiovascular parameter	A-686085				A-1048400			
	Dose (mg/kg i.v.)	0.3	1	3	Dose (mg/kg i.v.)	3	10	30
	Baseline	% of vehicle			Baseline	% of vehicle		
Mean arterial pressure (mmHg)	95 ± 5	87 ± 3*	63 ± 3*	58[a]	96 ± 3	93 ± 4	96 ± 6	92 ± 8
Heart rate (beats/min)	371 ± 14	100 ± 1	99 ± 2	99[a]	344 ± 6	100 ± 1	96 ± 1	88 ± 10
Left ventricular contractility (mmHg/s)	6988 ± 222	110 ± 3	105 ± 4	105[a]	6671 ± 294	104 ± 3	105 ± 5	110 ± 6
Plasma levels (mg/ml)		0.1 ± 0.04	0.3 ± 0.06	0.7 ± 0.1		1.0 ± 1.0	4.9 ± 1.5	11.9 ± 0.8

Male Sprague–Dawley rats were anesthetized with Inactin, instrumented and allowed to recover and stabilize. Following a 30 min baseline period compound prepared in PEG400 (1 ml/kg) was infused at 0.3, 1.0 and 3.0 mg/kg/30 min for A-686085 and 3.0, 10 and 30 mg/kg/30 min for A-1048400 by intravenous administration. The mean arterial pressure (mmHg), heart rate (beats/min) and left ventricular contractility (mmHg/s) were measured and the % of vehicle effect calculated. Peak plasma levels (μg/ml) were determined at the end of each dosing period using HPLC and mass spectrometry. Data are presented as mean ± SEM.

[a] Due to significant drops in mean arterial pressure induced by A-686085 at 3 mg/kg only a single rat was assessed therefore no SEM is shown for this dose.

* $p < 0.05$ vs. vehicle.

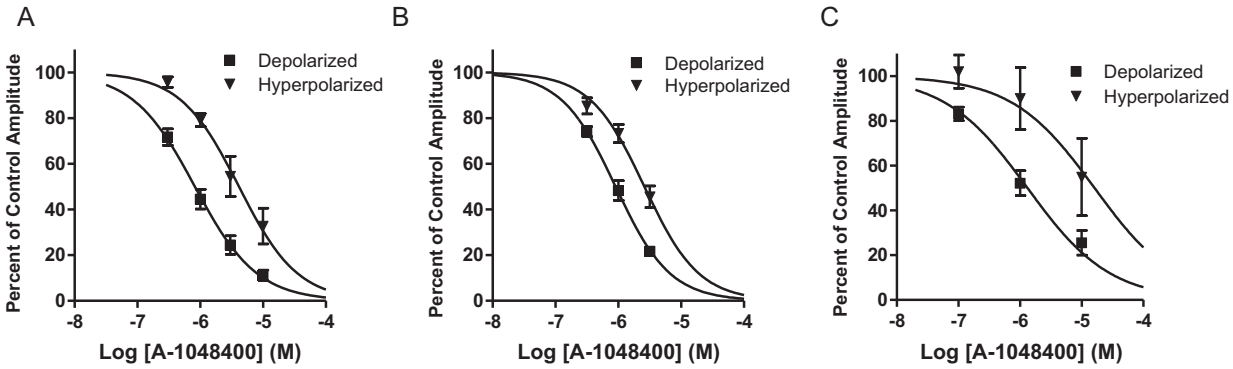

Fig. 4. A-1048400 blocks recombinant human calcium channels in a voltage-dependent fashion. The ability of A-1048400 to block human (A) N-type, (B) T-type, and (C) P/Q-type Ca^{2+} channels under hyperpolarized (▼) and depolarized, inactivating conditions (■) was determined by whole-cell patch clamp recordings. To assess closed state inhibition, cells were voltage clamped at hyperpolarized membrane potentials of −110 mV for T-type channels or −120 mV for N- and P/Q-type channels. To assess inactivated state inhibition, cells were voltage clamped at −70 to −75 mV for T-type channels, −80 mV for N-type channels and −90 mV for P/Q-type channels. Data are presented as a percent of control amplitude ± SEM before the addition of 3–4 increasing concentrations of A-1048400. Data shown are representative of at least n = 3–4 different cells.

−65 mV, A-1048400 blocked native N-type Ca^{2+} channels with an IC_{50} = 3.0 μM (95% CI: 2.0–4.5 μM; Fig. 5A; Table 2). This holding potential maintains native N-type Ca^{2+} channels at a less inactivated state relative to the recordings using recombinantly expressed human channels but was necessary for stable measurements of the native N-type current. At native low-voltage activated (T-type) Ca^{2+} channels in rat DRG neurons, A-1048400 blocked the channel in the inactivated state with an IC_{50} = 1.6 μM (95% CI: 1.3–1.9 μM; Fig. 5B; Table 2) which is comparable to its activity at human $Ca_v3.2$ channels described above.

3.6. Selectivity of A-1048400

The pharmacological activity of A-1048400 was evaluated across a panel of 80 different cell surface receptors, enzymes, and ion channels (CEREP Poitiers, France) [45]. A-1048400 had little or no activity (IC_{50} values > 10 μM) in all assays except the neuropeptide Y2 binding assay which gave a Ki = 0.97 μM.

3.7. A-1048400 reduced nociceptive, inflammatory and neuropathic pain in experimental models

In the MIA-induced osteoarthritis pain model, significant reduction in grip force was observed 21 days following injection of MIA directly into the hindlimb knee joint. In naïve (control) rats hindlimb grip force was 1046 ± 18 CF_{max}/kg body weight. Hindlimb grip force was significantly reduced ($p < 0.01$) to 403 ± 39 CF_{max}/kg body weight at 3 weeks following MIA-injection. A-1048400 dose-dependently reversed hindlimb grip force deficit with an ED_{50} = 8.9 mg/kg (95% CI: 6.7–12.8 mg/kg;

Table 2
Electrophysiological characterization of A-1048400 at Ca^{2+} channel subtypes.

Subtype	Species	IC_{50} closed state (μM)	IC_{50} inactivated state (μM)
$Ca_v2.1$	Human	16.1 (95% CI: 4.7–56)	1.3 (95% CI: 0.5–3.4)
$Ca_v2.2$	Human	4.1 (95% CI: 2.8–6.1)	0.8 (95% CI: 0.66–1.0)
$Ca_v3.2$	Human	2.6 (95% CI: 2–3.4)	0.9 (95% CI: 0.8–1.0)
T-type-DRG	Rat		1.6 (95% CI: 1.3–1.9)
HVA-DRG	Rat		3.0 (95% CI: 2.0–4.5)

The inhibition of several different voltage-dependent Ca^{2+} channels by A-1048400 was measured using whole-cell patch clamp analysis. Each Ca^{2+} channel subtype and species is shown. In recombinant cell lines, inhibition was measured under hyperpolarized (−120 mV for $Ca_v2.1$; −100 mV for $Ca_v2.2$; −100 mV for $Ca_v3.2$) and depolarized, inactivated (−90 mV for $Ca_v2.1$; −80 mV for $Ca_v2.2$; −70 to −75 mV for $Ca_v3.2$) conditions for each of the channels and data from at least 3–4 cells per condition and 95% confidence intervals are given for each data set. DRG: dorsal root ganglion neurons.

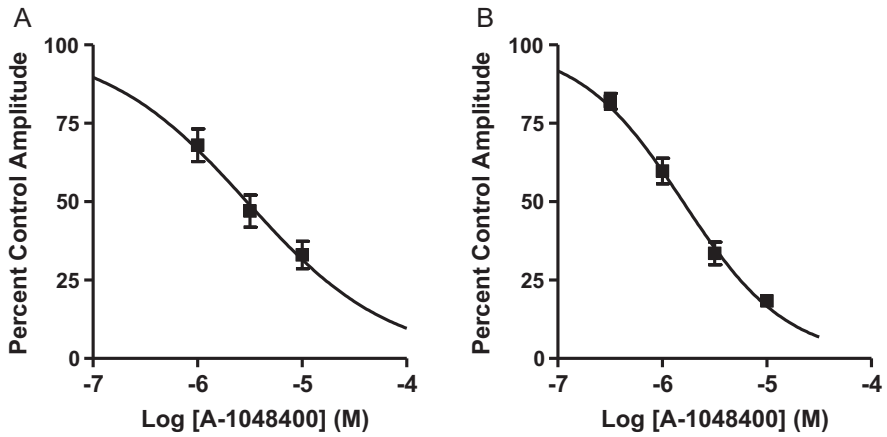

Fig. 5. A-1048400 blocks native Ca^{2+} currents in rat DRG neurons. (A) Inhibition of N-type Ca^{2+} currents in DRG neurons by A-1048400 were performed using whole-cell voltage clamp recordings at −60 to −65 mV. To minimize the contribution from non N-type Ca^{2+} channels 1 μM nifedipine, 150 nM SNX-482 and 300 nM ω-Agatoxin-IVa were included in the external solution to block L-type, R-type and P/Q-type Ca^{2+} channels, respectively. DRG neurons used in these recordings had a cell diameter between 25 and 35 μm. (B) Inhibition measurements of T-type calcium currents in DRG neurons by A-1048400 were measured using whole-cell voltage-clamp recordings at −75 mV (inactivated state) and were from DRG neurons with a cell diameter between 35–42 μm. Data are presented as a percent of control amplitude ± SEM before the addition of 2–4 increasing concentrations of A-1048400. n = 4–5 (N-type) or 3–7 (T-type) for each data point.

Fig. 6; n = 12 per group), with full efficacy was observed at 30 mg/kg.

In the CFA model of subchronic inflammatory pain, significant mechanical allodynia (PWT: 4.3 ± 0.3 g) developed 48 h following CFA injection. A-1048400 dose dependently reversed mechanical allodynia, with an ED_{50} = 38 mg/kg (95% CI: 18–100 mg/kg; Fig. 7; n = 12 per group).

In the SNL model of neuropathic pain, significant mechanical allodynia (PWT: 2.9 ± 0.1 g) was induced following ligation of the L5 and L6 spinal nerves. A-1048400 reversed mechanical allodynia in SNL rats with an ED_{50} = 15 mg/kg (95% CI: 9–23 mg/kg; Fig. 8A; n = 12 per group). In the model of CCI-induced neuropathic pain, significant mechanical allodynia (PWT: 3.6 ± 0.2 g) was observed 14 days following injury. A-1048400 dose-dependently reversed mechanical allodynia in CCI rats, with an estimated ED_{50} = 53 mg/kg (95% CI: 34–73 mg/kg; Fig. 8B; n = 12 per group). Collectively these data demonstrate that voltage-dependent blockade of neuronal Ca^{2+} channels by A-1048400 produced significant antinociception in experimental models of chronic nociceptive, inflammatory, and neuropathic pain.

3.8. A-1048400 has minimal effects on motor coordinating performance

A-1048400 produced no significant deficits in balance or motor coordinating performance at doses up to 300 mg/kg p.o. as assessed in the Rotarod assay (Fig. 9A; n = 6 per group). The corresponding plasma level for A-1048400 at a dose of 300 mg/kg, p.o. was 2.5 μg/ml. For comparison, haperidol (3.8 mg/kg) was assessed as a positive control and produced significant deficits in motor performance ($p < 0.01$). In the modified edge test, A-1048400 did not induce significant effects at doses up to 300 mg/kg (Fig. 9B; n = 6 per group). The non-competitive NMDA receptor antagonist MK-801 (0.1 mg/kg) was used as a positive control and produced significant motor impairment in this assay ($p < 0.001$).

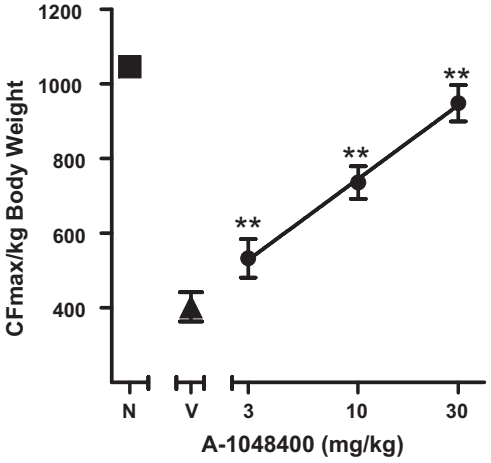

Fig. 6. Effect of A-1048400 on MIA-induced osteoarthritic pain. A-1048400 was administered orally at 3, 10 and 30 mg/kg 21 days following MIA-injection. Grip force was assessed 60 min after compound treatment. Data (●) represent mean ± SEM, $^{**}p < 0.01$ (n = 12 per group) compared with vehicle-treated rats. CF_{max} is the maximum compressive force. Data is also shown for naïve (■) and vehicle (▲) treated. *N*: naïve; *V*: vehicle.

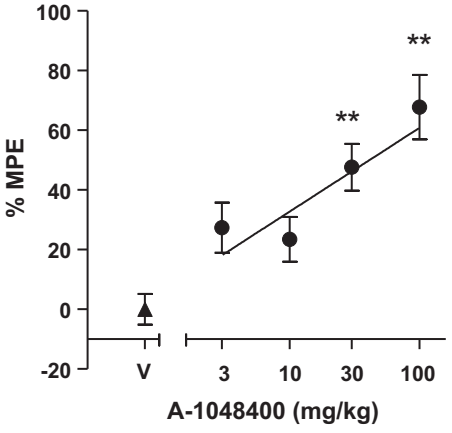

Fig. 7. Effect of A-1048400 on CFA-induced inflammatory pain. A-1048400 was administered orally at 3, 10, 30 and 100 mg/kg 48 h following CFA-injection. Mechanical allodynia was assessed 60 min after compound treatment. Data (●) are expressed as the percentage of maximal possible effect (% MPE) ± SEM, $^{**}p < 0.01$ vs. vehicle-treated rats (n = 12 per group). 100% MPE equals 15 g force measured using von Frey hairs as detailed in the methods section. Data is also shown for vehicle (▲) treated rats. V: vehicle.

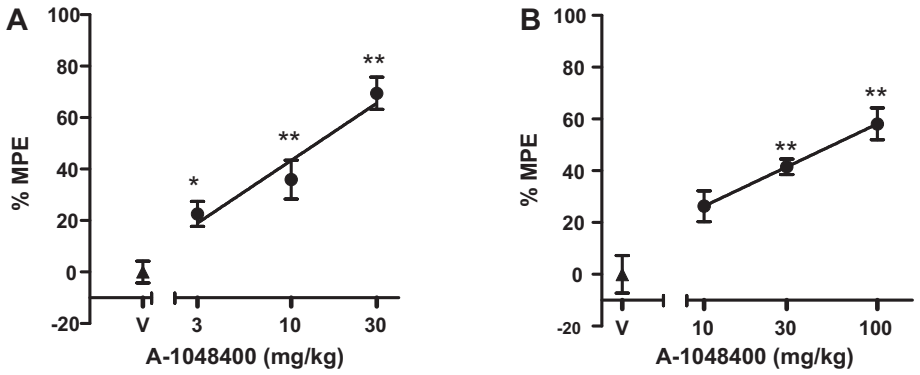

Fig. 8. Effects of A-1048400 on neuropathic pain. (A) A-1048400 was administered orally at 3, 10 and 30 mg/kg in the SNL-induced neuropathic pain model, and mechanical allodynia was assessed 60 min after compound administration. (B) A-1048400 was p.o. administered at 10, 30 and 100 mg/kg in CCI-induced neuropathic pain model, and mechanical allodynia was assessed 60 min after compound administration. Data (●) are expressed as the percentage of maximal possible effect (% MPE) ± SEM, $^{**}p < 0.01$ vs. vehicle-treated rats (n = 12 per group). 100% MPE equals 15 g force measured using von Frey hairs as detailed in the methods section. Data is also shown for vehicle (▲) treated rats. V: vehicle.

4. Discussion

The present study describes the identification of two structurally related neuronal Ca^{2+} channel blockers, A-686085 and A-1048400 that have similar activity at N-type Ca^{2+} channels and demonstrate comparable dose-dependent antinociception in the Cap-SMH model following systemic administration. However, both compounds differ significantly in their ability to block L-type Ca^{2+} channels as assessed in a rat aorta tissue relaxation assay. The physiological significance of this differential activity at N-type and L-type Ca^{2+} channels was demonstrated by the fact that A-686085 produced profound effects on MAP at antinociceptive plasma concentrations while A-1048400 did not alter hemodynamic function at plasma levels at least 14-fold above those required to reduce nociception in the Cap-SMH model.

A-1048400 was studied further to characterize its *in vitro* and *in vivo* pharmacology. In electrophysiology studies, A-1048400 blocked recombinant human and native rat N-, T, and P/Q-type Ca^{2+} channels in a voltage-dependent fashion with similar potencies. A-1048400 also produced dose-dependent antinociception across animal models of nociceptive, inflammatory and neuropathic pain demonstrating that blocking these channels in a state-dependent manner leads to significant analgesia. In the neuropathic pain models, A-1048400 was approximately 3-fold more potent in the SNL model compared to the CCI model. While the specific reason for this difference in antinociceptive potency in not known, these data may indicate a greater relative contribution of neuronal calcium channels in the pain associated with frank nerve injury (SNL) compared to the inflammatory neuritis associated with the CCI model [47,52]. In addition to its lack of effects on cardiovascular function, A-1048400 did not alter balance or rotarod performance at doses up to 300 mg/kg likely due to the limited CNS penetration observed with this compound.

The antinociceptive activity of A-1048400 is consistent with the analgesic effects of the peptide N-type Ca^{2+} channel blocker, ziconotide that effectively attenuates pain responses in experimental pain models [13–17] and in intractable chronic pain patients following intrathecal administration [19,20]. There are however significant differences between ziconotide and A-1048400. Ziconotide selectively blocks N-type Ca^{2+} channels in a state-independent manner with similar affinity for the open/resting/inactivated states of the channel [57]. In contrast A-1048400 is a state-dependent blocker that preferentially binds to the inactivated state of the channel and stabilizes the channel in this conformation. Another difference between these two agents is that ziconotide requires intrathecal administration to achieve robust analgesic efficacy, while A-1048400 is orally bioavailable and has limited CNS penetration yet provides a similar analgesic

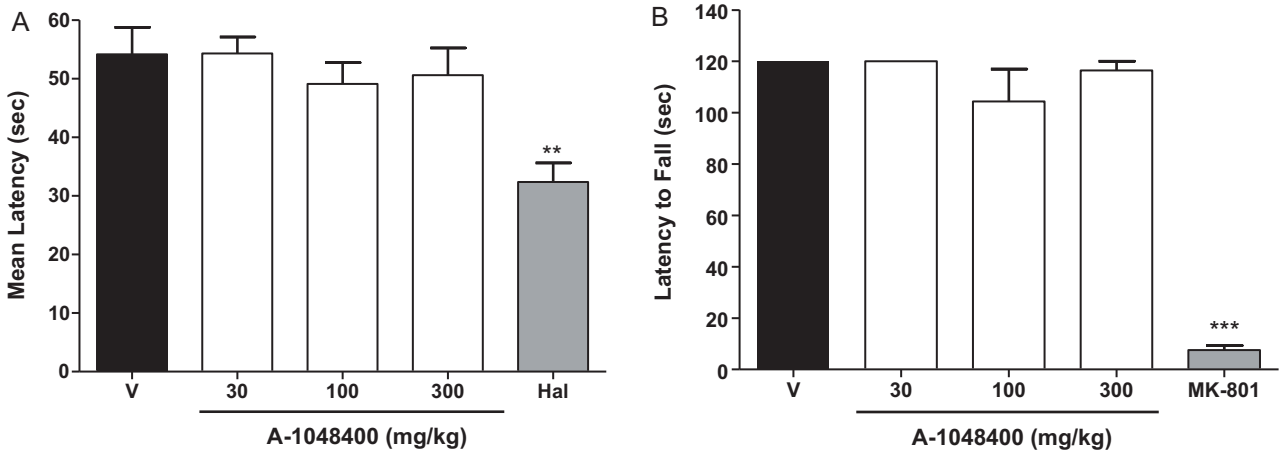

Fig. 9. Effects of A-1048400 on motor coordination in naïve rats. (A) A-1048400 was administered orally at 30, 100 and 300 mg/kg, with haloperidol (Hal) administered at 3.7 mg/kg (p.o.) as positive control. Fall latency (s) was assessed 60 min after compound treatment in the Rotarod assay. (B) A-1048400 was administered orally at 30, 100 and 300 mg/kg, with MK-801 administered at 0.1 mg/kg (p.o.) as positive control. Latency to fall (s) was assessed 60 min after compound treatment in edge assay. Data represent mean ± SEM, $^{**}p < 0.01$ or $^{***}p < 0.001$ vs. vehicle-treated rats (V, n = 6 per group).

profile in preclinical pain models. Additionally, A-1048400 also blocks T- and P/Q-type Ca^{2+} channels unlike ziconotide that may further contribute to its antinociceptive activity [21,58].

The role of T-type Ca^{2+} channels in nociception is well characterized in experimental pain models [21]. For example, intrathecal delivery of a $Ca_v3.2$ specific antisense oligonucleotide that reduced the levels of $Ca_v3.2$ by 80–90% in DRG neurons in the peripheral nervous system completely reversed mechanical hyperalgesia in the CCI model of neuropathic pain [26]. The role of P/Q-type Ca^{2+} channel in nociception is still emerging and insights have arisen from knockout mice studies [59]. While homozygote knockout $Ca_v2.1$ mice have severe neurological dysfunctions and typically die 4 weeks after birth [60,61], adult heterozygous $Ca_v2.1^{+/-}$ mice show reduced licking responses during the second phase of the formalin model and reduced mechanical allodynia in the CCI model of neuropathic pain [58].

N-type Ca^{2+} channels are also involved in cardiovascular function and are expressed on sympathetic neurons that innervate the vasculature and modulate hemodynamic tone [62,63]. Systemic blockade of N-type Ca^{2+} channels with selective peptide toxins such as ω-conotoxin GVIA or ziconotide, leads to dose-related vasorelaxation and a marked decrease in MAP [64]. Since ziconotide is a potent, poorly reversible N-type Ca^{2+}channel state-independent blocker [57] and does not cross the blood brain barrier, systemic administration of the peptidic antagonist produces robust hypotension without significant analgesia [14]. In contrast, A-1048400 blocks neuronal Ca^{2+} channels in a voltage-dependent (state-dependent) fashion and does not significantly alter hemodynamic function in the rat at plasma concentrations well above those necessary for robust antinociception in the rat. Additionally, A-1048400 did not produce significant effects in either the rotarod assay or the edge test at plasma levels significantly higher than those required to produce antinociception. Following nerve injury or trauma, sensory neurons become sensitized and hyperexcitable generating higher frequencies of action potential generation [65,66]. Voltage-dependent blockers on neuronal ion channels that interact with specific states of the channel may preferentially modulate hyperactive neurons while having comparatively minimal effects on normal neuronal activity [28–30]. Additional pharmacological support for this hypothesis as a viable analgesic mechanism has been recently provided by the identification of several novel voltage-dependent Ca^{2+} and Na^{+} channel blockers that effectively reduce chronic pain states in the absence of significant cardiovascular or CNS side-effects in preclinical models. NP118809 and NP078585 are neuronal Ca^{2+} channel blockers that block N- T- and P/Q-type subtypes and effectively reduce nociception in the formalin model of persistent pain [67]. NP118809 also attenuates mechanical and thermal nociception in the rat SNL model of neuropathic pain [68]. The analgesic efficacy observed with these molecules occurred in the absence of overt peripheral or central side effects [29,67,68]. TROX-1 is a voltage-dependent blocker of N-, P/Q- and R-type Ca^{2+} channels, that attenuates persistent neuropathic and inflammatory pain in experimental models without producing significant deleterious effects on CNS or cardiovascular function TTA-P2 is another voltage-dependent, CNS penetrant, and selective T-type Ca^{2+} channel blocker that was recently identified [70]. TTA-P2 reduces pain responses in phase I and 2 of the formalin model of persistent pain [71]. Furthermore, TTA-P2 attenuated thermal hyperalgesia in streptozocin induced diabetic rats but had no effects on nociceptive responses in healthy animals [71]. These data demonstrate that selectively blocking T-type Ca^{2+} channels provides attenuation of nociceptive responses in certain chronic pain states. Z123212 is another recently described blocker of neuronal Ca^{2+} and Na^{+} channels that selectively stabilizes the slow-inactivation states of these channels while having little or no significant affinity for channels in the resting state [72]. Like the other ion channel blockers described above, Z123212 produces dose-dependent antinociception following peripheral nerve injury without significantly altering cardiovascular or CNS function [72].

The present study highlights two important properties that are likely required for small molecule Ca^{2+} channel blockers to effectively reduce pathological nociception in the absence of untoward effects on CNS and cardiovascular function. The voltage-dependent activity of A-1048400 in blocking N-type and T-type Ca^{2+} channels, coupled with a relative lack of activity at L-type Ca^{2+} channels are necessary to achieve robust antinociceptive activity across multiple chronic pain models while preserving normal psychomotor and cardiovascular function. Since A-1048400 is a nonselective blocker of N-, T-, and P/Q-type channels, the individual contributions of each channel isoform to the observed antinocicpetive effects of A-1048400 cannot be determined. However, the present data are consistent with data reported for other recently described nonselective neuronal ion channel blockers [67,69,72] and illustrate the potential feasibility and utility of developing such compounds for the treatment of chronic pain.

Since the diphenylmethylpiperazine pharmacophore is well known as a Ca^{2+} channel blocker (Doherty et al., submitted for publication), the discovery of the diphenyl lactam moiety offers a new approach for modulating the activity of this series at individual Ca^{2+} channel subunits. The present data comparing the pharmacology of A-686085 and A-1048400 show that activity at L-type Ca^{2+} channels can readily be reduced in the diphenyl lactam series and that this effect is associated with reduced effects on hemodynamic function in the rat. As noted above, several novel small molecule blockers have emerged that are efficacious in experimental models of neuropathic pain and show improved therapeutic margins for cardiovascular and psychomotor liabilities [69,72]. The present demonstration of the ability of A-1048400 to produce robust antinociception in models of inflammatory and osteoarthritis pain extends the potential therapeutic utility of neuronal Ca^{2+} channel blockers in chronic pain states.

Acknowledgments

We would like to acknowledge Dr. Char-Chang Shieh, Dr. Di Zhang, Marian Namovic, Rama Thimmapaya, Rosalind Helfrich and Jill Wetter for their technical contributions to these studies. We would also like to acknowledge Dr. Carol Surowy and Dr. Diana Donnelly-Roberts for their helpful discussions on the data presented in this manuscript.

References

[1] Catterall WA. Ion channel voltage sensors: structure, function, and pathophysiology. Neuron 2010;67:915–28.
[2] Catterall WA. Structure and regulation of voltage-gated Ca^{2+} channels. Annual Review of Cell and Developmental Biology 2000;16:521–55.
[3] Zamponi GW, Lewis RJ, Todorovic SM, Arneric SP, Snutch TP. Role of voltage-gated calcium channels in ascending pain pathways. Brain Research Reviews 2009;60:84–9.
[4] Bao J, Li JJ, Perl ER. Differences in Ca^{2+} channels governing generation of miniature and evoked excitatory synaptic currents in spinal laminae I and II. Journal of Neuroscience 1998;18:8740–50.
[5] Heinke B, Balzer E, Sandkuhler J. Pre- and postsynaptic contributions of voltage-dependent Ca^{2+} channels to nociceptive transmission in rat spinal lamina I neurons. European Journal of Neuroscience 2004;19:103–11.
[6] Urban MO, Ren K, Sablad M, Park KT. Medullary N-type and P/Q-type calcium channels contribute to neuropathy-induced allodynia. Neuroreport 2005; 16:563–6.
[7] Cizkova D, Marsala J, Lukacova N, Marsala M, Jergova S, Orendacova J, et al. Localization of N-type Ca^{2+} channels in the rat spinal cord following chronic constrictive nerve injury. Experimental Brain Research Experimentelle Hirnforschung 2002;147:456–63.
[8] Luo ZD, Chaplan SR, Higuera ES, Sorkin LS, Stauderman KA, Williams ME, et al. Upregulation of dorsal root ganglion (alpha)2(delta) calcium channel subunit

and its correlation with allodynia in spinal nerve-injured rats. Journal of Neuroscience 2001;21:1868–75.
[9] Newton RA, Bingham S, Case PC, Sanger GJ, Lawson SN. Dorsal root ganglion neurons show increased expression of the calcium channel alpha2delta-1 subunit following partial sciatic nerve injury. Brain Research 2001;95:1–8.
[10] Hatakeyama S, Wakamori M, Ino M, Miyamoto N, Takahashi E, Yoshinaga T, et al. Differential nociceptive responses in mice lacking the alpha(1B) subunit of N-type $Ca^{(2+)}$ channels. Neuroreport 2001;12:2423–7.
[11] Kim C, Jun K, Lee T, Kim SS, McEnery MW, Chin H, et al. Altered nociceptive response in mice deficient in the alpha(1B) subunit of the voltage-dependent calcium channel. Molecular and Cellular Neurosciences 2001;18:235–45.
[12] Saegusa H, Kurihara T, Zong S, Kazuno A, Matsuda Y, Nonaka T, et al. Suppression of inflammatory and neuropathic pain symptoms in mice lacking the N-type Ca^{2+} channel. The EMBO journal 2001;20:2349–56.
[13] Wang YX, Gao D, Pettus M, Phillips C, Bowersox SS. Interactions of intrathecally administered ziconotide, a selective blocker of neuronal N-type voltage-sensitive calcium channels, with morphine on nociception in rats. Pain 2000;84:271–81.
[14] Bowersox SS, Gadbois T, Singh T, Pettus M, Wang YX, Luther RR. Selective N-type neuronal voltage-sensitive calcium channel blocker, SNX-111, produces spinal antinociception in rat models of acute, persistent and neuropathic pain. Journal of Pharmacology and Experimental Therapeutics 1996;279:1243–9.
[15] Yamamoto T, Sakashita Y. Differential effects of intrathecally administered N- and P-type voltage-sensitive calcium channel blockers upon two models of experimental mononeuropathy in the rat. Brain Research 1998;794:329–32.
[16] Wang YX, Pettus M, Gao D, Phillips C, Scott Bowersox S. Effects of intrathecal administration of ziconotide, a selective neuronal N-type calcium channel blocker, on mechanical allodynia and heat hyperalgesia in a rat model of postoperative pain. Pain 2000;84:151–8.
[17] Smith MT, Cabot PJ, Ross FB, Robertson AD, Lewis RJ. The novel N-type calcium channel blocker, AM336, produces potent dose-dependent antinociception after intrathecal dosing in rats and inhibits substance P release in rat spinal cord slices. Pain 2002;96:119–27.
[18] Rauck RL, Wallace MS, Leong MS, Minehart M, Webster LR, Charapata SG, et al. A randomized, double-blind, placebo-controlled study of intrathecal ziconotide in adults with severe chronic pain. Journal of Pain and Symptom Management 2006;31:393–406.
[19] Staats PS, Yearwood T, Charapata SG, Presley RW, Wallace MS, Byas-Smith M, et al. Intrathecal ziconotide in the treatment of refractory pain in patients with cancer or AIDS: a randomized controlled trial. Journal of the American Medical Association 2004;291:63–70.
[20] Wallace MS. Ziconotide: a new nonopioid intrathecal analgesic for the treatment of chronic pain. Expert Review of Neurotherapeutics 2006;6:1423–8.
[21] Todorovic SM, Jevtovic-Todorovic V. T-type voltage-gated calcium channels as targets for the development of novel pain therapies. British Journal of Pharmacology 2011;163:484–95.
[22] Perez-Reyes E. Molecular physiology of low-voltage-activated t-type calcium channels. Physiological Reviews 2003;83:117–61.
[23] Todorovic SM, Jevtovic-Todorovic V. The role of T-type calcium channels in peripheral and central pain processing. CNS & Neurological Disorders Drug Targets 2006;5:639–53.
[24] Jagodic MM, Pathirathna S, Nelson MT, Mancuso S, Joksovic PM, Rosenberg ER, et al. Cell-specific alterations of T-type calcium current in painful diabetic neuropathy enhance excitability of sensory neurons. Journal of Neuroscience 2007;27:3305–16.
[25] Jagodic MM, Pathirathna S, Joksovic PM, Lee W, Nelson MT, Naik AK, et al. Upregulation of the T-type calcium current in small rat sensory neurons after chronic constrictive injury of the sciatic nerve. Journal of Neurophysiology 2008;99:3151–6.
[26] Bourinet E, Alloui A, Monteil A, Barrere C, Couette B, Poirot O, et al. Silencing of the $Ca_v3.2$ T-type calcium channel gene in sensory neurons demonstrates its major role in nociception. EMBO Journal 2005;24:315–24.
[27] Choi S, Na HS, Kim J, Lee J, Lee S, Kim D, et al. Attenuated pain responses in mice lacking $Ca_{(v)}3.2$ T-type channels. Genes Brain and Behavior 2007;6:425–31.
[28] McGivern JG, McDonough SI. Voltage-gated calcium channels as targets for the treatment of chronic pain. Current Drug Targets 2004;3:457–78.
[29] Snutch TP. Targeting chronic and neuropathic pain: the N-type calcium channel comes of age. NeuroRx 2005;2:662–70.
[30] Winquist RJ, Pan JQ, Gribkoff VK. Use-dependent blockade of $Ca_v2.2$ voltage-gated calcium channels for neuropathic pain. Biochemical Pharmacology 2005;70:489–99.
[31] Bean BP. Nitrendipine block of cardiac calcium channels: high-affinity binding to the inactivated state. Proceedings of the National Academy of Sciences of the United States of America 1984;81:6388–92.
[32] Reger TS. T-type calcium channel blockers. In: 237th ACS meeting. Salt Lake City: ACS; 2009. p. 57–65.
[33] Catterall WA. Common modes of drug action on Na channels: local anesthetics, antiarrhymics and anticonvulsants. Trends in Pharmacological Sciences 1987;8:57–65.
[34] Gould RJ, Murphy KM, Reynolds IJ, Snyder SH. Antischizophrenic drugs of the diphenylbutylpiperidine type act as calcium channel antagonists. Proceedings of the National Academy of Sciences of the United States of America 1983;80:5122–5.
[35] Vortherms TA, Swensen AM, Niforatos W, Limberis JT, Neelands TR, Janis RS, et al. Comparative analysis of inactivated-state block of N-type ($Ca_{(v)}2.2$) calcium channels. Inflammation Research 2011;60:683–93.
[36] Lubin ML, Reitz TL, Todd MJ, Flores CM, Qin N, Xin H. A nonadherent cell-based HTS assay for N-type calcium channel using calcium 3 dye. Assay and Drug Development Technologies 2006;4:689–94.
[37] Xie X, Van Deusen AL, Vitko I, Babu DA, Davies LA, Huynh N, et al. Validation of high throughput screening assays against three subtypes of $Ca_{(v)}3$ T-type channels using molecular and pharmacologic approaches. Assay and Drug Development Technologies 2007;5:191–203.
[38] Buckner SA, Oheim KW, Morse PA, Knepper SM, Hancock AA. Alpha 1-adrenoceptor-induced contractility in rat aorta is mediated by the alpha 1D subtype. European Journal of Pharmacology 1996;297:241–8.
[39] Lin Y, McDonough SI, Lipscombe D. Alternative splicing in the voltage-sensing region of N-Type $Ca_v2.2$ channels modulates channel kinetics. Journal of Neurophysiology 2004;92:2820–30.
[40] Scroggs RS, Fox AP. Calcium current variation between acutely isolated adult rat dorsal root ganglion neurons of different size. Journal of Physiology 1992;445:639–58.
[41] Cardenas CG, Del Mar LP, Scroggs RS. Variation in serotonergic inhibition of calcium channel currents in four types of rat sensory neurons differentiated by membrane properties. Journal of Neurophysiology 1995;74:1870–9.
[42] Mery PF, Hove-Madsen L, Mazet JL, Hanf R, Fischmeister R. Binding constants determined from Ca^{2+} current responses to rapid applications and washouts of nifedipine in frog cardiac myocytes. Journal of Physiology 1996;494(Pt 1):105–20.
[43] Newcomb R, Szoke B, Palma A, Wang G, Chen X, Hopkins W, et al. Selective peptide antagonist of the class E calcium channel from the venom of the tarantula Hysterocrates gigas. Biochemistry 1998;37:15353–62.
[44] Mintz IM, Venema VJ, Swiderek KM, Lee TD, Bean BP, Adams ME. P-type calcium channels blocked by the spider toxin omega-Aga-IVA. Nature 1992;355:827–9.
[45] El Kouhen R, Surowy CS, Bianchi BR, Neelands TR, McDonald HA, Niforatos W, et al. A-425619 [1-isoquinolin-5-yl-3-(4-trifluoromethyl-benzyl)-urea], a novel and selective transient receptor potential type V1 receptor antagonist, blocks channel activation by vanilloids, heat, and acid. Journal of Pharmacology and Experimental Therapeutics 2005;314:400–9.
[46] Liu G, Zhao H, Liu B, Xin Z, Liu M, Serby MD, et al. Hemodynamic effects of potent and selective JNK inhibitors in anesthetized rats: implication for targeting protein kinases in metabolic diseases. Bioorganic & Medicinal Chemistry Letters 2007;17:495–500.
[47] Joshi SK, Hernandez G, Mikusa JP, Zhu CZ, Zhong C, Salyers A, et al. Comparison of antinociceptive actions of standard analgesics in attenuating capsaicin and nerve-injury-induced mechanical hypersensitivity. Neuroscience 2006;143:587–96.
[48] Chaplan SR, Bach FW, Pogrel JW, Chung JM, Yaksh TL. Quantitative assessment of tactile allodynia in the rat paw. Journal of Neuroscience Methods 1994;53:55–63.
[49] Dixon WJ. Efficient analysis of experimental observations. Annual Review of Pharmacology Toxicology 1980;20:441–62.
[50] Chandran P, Pai M, Blomme EA, Hsieh GC, Decker MW, Honore P. Pharmacological modulation of movement-evoked pain in a rat model of osteoarthritis. European Journal of Pharmacology 2009;613:39–45.
[51] Kim SH, Chung JM. An experimental model for peripheral neuropathy produced by segmental spinal nerve ligation in the rat. Pain 1992;50:355–63.
[52] Bennett GJ, Xie YK. A peripheral mononeuropathy in rat that produces disorders of pain sensation like those seen in man. Pain 1988;33:87–107.
[53] Bannon AW, Decker MW, Curzon P, Buckley MJ, Kim DJ, Radek RJ, et al. ABT-594 [(R)-5-(2-azetidinylmethoxy)-2-chloropyridine]: a novel, orally effective antinociceptive agent acting via neuronal nicotinic acetylcholine receptors: II. In vivo characterization. Journal of Pharmacology and Experimental Therapeutics 1998;285:787–94.
[54] Carbone E, Sher E, Clementi F. Ca currents in human neuroblastoma IMR32 cells: kinetics, permeability and pharmacology. Pflugers Archiv 1990;416:170–9.
[55] Opie LH. Calcium channel antagonists, part I: fundamental properties: mechanisms, classification, sites of action. Cardiovascular Drugs and Therapy 1987;1:411–30 (sponsored by the International Society of Cardiovascular Pharmacotherapy).
[56] Valdivielso JM, Macias JF, Lopez-Novoa JM. Cardiovascular effects of elgodipine and nifedipine compared in anaesthetized rats. European Journal of Pharmacology 1997;335:193–8.
[57] Feng ZP, Doering CJ, Winkfein RJ, Beedle AM, Spafford JD, Zamponi GW. Determinants of inhibition of transiently expressed voltage-gated calcium channels by omega-conotoxins GVIA and MVIIA. Journal of Biological Chemistry 2003;278:20171–8.
[58] Luvisetto S, Marinelli S, Panasiti MS, D'Amato FR, Fletcher CF, Pavone F, et al. Pain sensitivity in mice lacking the $Ca_{(v)}2.1$alpha1 subunit of P/Q-type Ca^{2+} channels. Neuroscience 2006;142:823–32.
[59] Pietrobon D. Function and dysfunction of synaptic calcium channels: insights from mouse models. Current Opinion in Neurobiology 2005;15:257–65.
[60] Jun K, Piedras-Renteria ES, Smith SM, Wheeler DB, Lee SB, Lee TG, et al. Ablation of P/Q-type $Ca^{(2+)}$ channel currents, altered synaptic transmission, and progressive ataxia in mice lacking the alpha(1A)-subunit. Proceedings of the National Academy of Sciences of the United States of America 1999;96:15245–50.
[61] Fletcher CF, Tottene A, Lennon VA, Wilson SM, Dubel SJ, Paylor R, et al. Dystonia and cerebellar atrophy in Cacna1a null mice lacking P/Q calcium channel activity. FASEB Journal 2001;15:1288–90.

[62] Hirning LD, Fox AP, McCleskey EW, Olivera BM, Thayer SA, Miller RJ, et al. Dominant role of N-type Ca^{2+} channels in evoked release of norepinephrine from sympathetic neurons. Science (New York NY) 1988;239:57–61.
[63] Molderings GJ, Likungu J, Gothert M. N-Type calcium channels control sympathetic neurotransmission in human heart atrium. Circulation 2000;101: 403–7.
[64] Bowersox SS, Singh T, Nadasdi L, Zukowska-Grojec Z, Valentino K, Hoffman BB. Cardiovascular effects of omega-conopeptides in conscious rats: mechanisms of action. Journal of Cardiovascular Pharmacology 1992;20:756–64.
[65] Zhang JM, Song XJ, LaMotte RH. Enhanced excitability of sensory neurons in rats with cutaneous hyperalgesia produced by chronic compression of the dorsal root ganglion. Journal of Neurophysiology 1999;82:3359–66.
[66] Latremoliere A, Woolf CJ. Central sensitization: a generator of pain hypersensitivity by central neural plasticity. Journal of Pain 2009;10:895–926.
[67] Zamponi GW, Feng ZP, Zhang L, Pajouhesh H, Ding Y, Belardetti F, et al. Scaffold-based design and synthesis of potent N-type calcium channel blockers. Bioorganic & Medicinal Chemistry Letters 2009;19:6467–72.
[68] Pajouhesh H, Feng ZP, Ding Y, Zhang L, Pajouhesh H, Morrison JL, et al. Structure-activity relationships of diphenylpiperazine N-type calcium channel inhibitors. Bioorganic & Medicinal Chemistry Letters 2010;20:1378–83.
[69] Abbadie C, McManus OB, Sun SY, Bugianesi RM, Dai G, Haedo RJ, et al. Analgesic effects of a substituted N-triazole oxindole (TROX-1), a state-dependent, voltage-gated calcium channel 2 blocker. Journal of Pharmacology and Experimental Therapeutics 2010;334:545–55.
[70] Shipe WD, Barrow JC, Yang ZQ, Lindsley CW, Yang FV, Schlegel KA, et al. Design, synthesis, and evaluation of a novel 4-aminomethyl-4-fluoropiperidine as a T-type Ca2+ channel antagonist. Journal of Medicinal Chemistry 2008;51:3692–5.
[71] Choe W, Messinger RB, Leach E, Eckle VS, Obradovic A, Salajegheh R, et al. TTA-P2 is a potent and selective blocker of T-type calcium channels in rat sensory neurons and a novel antinociceptive agent. Molecular Pharmacology 2011; 80:900–10.
[72] Hildebrand ME, Smith PL, Bladen C, Eduljee C, Xie JY, Chen L, et al. A novel slow-inactivation-specific ion channel modulator attenuates neuropathic pain. Pain 2011;152:833–43.